

Excitonic condensation in a double-layer graphene system

Maxim Yu. Kharitonov^{1,2} and Konstantin B. Efetov²

¹Materials Science Division, Argonne National Laboratory, Argonne, IL 60439, USA

²Institut für Theoretische Physik III, Ruhr-Universität Bochum, 44780 Bochum, Germany

Abstract. The possibility of excitonic condensation in a recently proposed electrically biased double-layer graphene system is studied theoretically. The main emphasis is put on obtaining a reliable analytical estimate for the transition temperature into the excitonic state. As in a double-layer graphene system the total number of fermionic “flavors” is equal to $N = 8$ due to two projections of spin, two valleys, and two layers, the large- N approximation appears to be especially suitable for theoretical investigation of the system. On the other hand, the large number of flavors makes screening of the bare Coulomb interactions very efficient, which, together with the suppression of backscattering in graphene, leads to an extremely low energy of the excitonic condensation. It is shown that the effect of screening on the excitonic pairing is just as strong in the excitonic state as it is in the normal state. As a result, the value of the excitonic gap Δ is found to be in full agreement with the previously obtained estimate for the mean-field transition temperature T_c , the maximum possible value $\Delta^{\max}, T_c^{\max} \sim 10^{-7} \epsilon_F$ (ϵ_F is the Fermi energy) of both being in 1mK range for a perfectly clean system. This proves that the energy scale $\sim 10^{-7} \epsilon_F$ really sets the upper bound for the transition temperature and invalidates the recently expressed conjecture about the high-temperature first-order transition into the excitonic state. These findings suggest that, unfortunately, the excitonic condensation in graphene double-layers can hardly be realized experimentally.

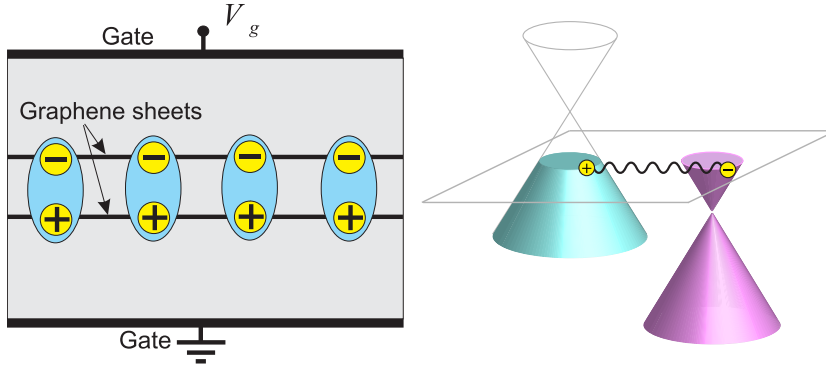


Figure 1. Excitonic condensate in a system of two spatially separated graphene layers. Electrons and holes in the layers are induced by applying the external gate voltage and the excitonic pairing is caused by the attractive interlayer Coulomb interaction.

1. Introduction

The idea of excitonic condensation in metallic systems was originally proposed [1] by Keldysh and Kopaev for semimetals with overlapping conduction and valence bands. They have shown that the attractive Coulomb interaction between electrons and holes leads to an instability towards formation of bound electron-hole pairs, analogous to the Cooper instability in superconductors. Somewhat later, Lozovik and Yudson suggested [2] that excitonic condensation could be realized in a double-layer system of spatially separated electrons and holes. If the layers are close enough to each other, the interlayer Coulomb interaction could still be appreciable, which would lead to coupling between electrons and holes.

It took a while after the proposals of Refs. [2] until the technology able to fabricate electron-hole bilayers has been developed. So far, experimental efforts have been mainly concentrated on the GaAs/ $\text{Al}_x\text{Ga}_{1-x}\text{As}$ double quantum well heterostructures and the evidence [3, 4, 5, 6, 7, 8, 9, 10] for excitonic condensation in such systems based on the investigation of the Coulomb drag [3, 4, 5] and photoluminescence spectra [6, 7, 8, 9, 10] is building. Another exciting phenomenon in the coupled semiconductor bilayers is the quantum Hall ferromagnetism [11, 12].

Besides semiconductor double quantum wells, what other materials and technology could be used for the search of the excitonic condensation? Graphene [13, 14, 15, 16, 17, 18, 19], an isolated atomic monolayer of carbon, could seem very attractive for this purpose. Indeed, quite recently several groups of authors [20, 21, 22, 23] proposed the following graphene-based setup (Fig. 1) as a candidate for the observation of the excitonic condensation. If one takes two graphene layers separated by an insulator, then electron doping in one layer and hole doping in the other can be obtained by applying external gate voltage. Analogously to the semiconductor quantum double wells, the interlayer Coulomb interaction would lead to coupling between electrons and holes.

What attractive properties does such graphene system have? First, the relatively high values of the Fermi energy $\epsilon_F \sim 0.3\text{eV}$ that can be achieved in graphene by

using electric gates [14] is an obvious advantage, since the condensation temperature is expected scale linearly with ϵ_F . Second, as any mismatch between the Fermi momenta of electrons and holes tends to suppress the condensate in the same way as the Zeeman splitting suppresses the conventional superconductivity, the nearly perfect matching of the electron and hole branches of the spectrum and the ability to fine-tune the carrier density become extremely important.

So, in terms of engineering properties, the double-layer graphene system (Fig. 1) could seem exceptionally attractive for realization of the excitonic condensation. However, before one proceeds with the fabrication of this system, an important theoretical question that should be answered is how high the temperature of transition to the excitonic state in such a setup could be.

Some seriously conflicting predictions have been reported in the literature on this matter. Initially, an estimate for the Berezinski-Kostelitz-Thouless (BKT) transition [24, 25] temperature in a double-layer graphene system was made in Refs. [22, 23]. Studying the problem numerically, the authors came to conclusion that the BKT temperature T_{KT}^* in this system could be very large,

$$T_{KT}^* \sim 0.1\epsilon_F. \quad (1)$$

With the Fermi energy $\epsilon_F \sim 0.3\text{eV}$, this would correspond to room temperatures, $T_{KT}^* \sim 300\text{K}$, which would be very encouraging for experimentalists.

Unfortunately, the estimate (1) for the transition temperature is too optimistic. As pointed out in Ref. [26] this result stemmed from the complete neglect of screening of the interlayer Coulomb interaction by the carriers in the layers in the analysis of Refs. [22, 23]. As the bare Coulomb interactions in graphene are not weak, it is not surprising that neglecting screening the transition temperature appeared to be only one order smaller than the Fermi energy ϵ_F . In Ref. [26] the mean field transition temperature T_c , at which the normal state becomes unstable towards electron-hole pair formation, was calculated. It was demonstrated that when screening is taken into account the highest possible value of the mean-field temperature turns out to be extremely small,

$$T_c^{\text{max}} \sim 10^{-7}\epsilon_F. \quad (2)$$

The reason for that is the large number $N = 8$ of “flavors” in a double-layer graphene system, which makes screening very efficient, and the suppression of backscattering in graphene due to the chiral nature of Dirac quasiparticles. These factors combined make the system effectively weakly interacting, and the transition temperature depends exponentially on the coupling constant in the weak-coupling regime. Since the thermal fluctuations of the order parameter in two dimensions can only suppress the superfluid properties of the system, the BKT transition temperature T_{KT} can be only smaller than the mean-field temperature (2).

Somewhat later, in Ref. [27], the authors of Ref. [22] presented arguments to justify the neglect of screening in Refs. [22, 23]. They argued that in the excitonic state screening had to be essentially suppressed due to the gap in the excitation spectrum.

This would mean that in the excitonic phase, at least at low enough temperatures, the interactions are not screened and the system is in the strong coupling regime of the bare Coulomb interactions. Therefore, the value of the gap $\Delta^*(T = 0)$ at zero temperature, when the suppression of screening is maximal, had to be of the same order as the initial estimate (1) for the BKT temperature,

$$\Delta^*(T = 0) \sim 0.1\epsilon_F. \quad (3)$$

A strong discrepancy between the small value (2) of the mean-field temperature and the large value (3) of the gap in the excitonic state implies, according to the authors of Ref. [27], that the system should undergo a first order transition at temperature $T \sim \Delta^*(T = 0)$, which would again correspond to room temperatures.

The purpose of this paper is to review in more detail the arguments leading to Eqs. (2) and (3) in order to understand which of the estimates for the transition temperature is finally correct. We will show that, in terms of its effect on the electron-hole pairing, screening in the excitonic state is just as strong as it is in the normal state. This is because a wide range of scattering momenta of electron and hole in a pair contributes to the value of the excitonic gap, whereas screening is suppressed only in a much narrower range of small momenta. As a result, an accurate analysis of the excitonic state yields essentially the same estimate

$$\Delta^{\max}(T = 0) \sim 10^{-7}\epsilon_F \quad (4)$$

for the highest possible value of the gap as the one obtained for the mean field temperature [Eq. (2)]. Therefore, the energy scale $\sim 10^{-7}\epsilon_F$ is the only one in the problem, no matter whether one considers the normal or excitonic state, and Eq. (2) is indeed the upper bound for the transition temperature into the excitonic state. This invalidates the argument of Ref. [27] about the high-temperature first-order transition. Considering that the excitonic condensate is sensitive to the impurity scattering, such a low transition temperature renders the observation of the excitonic condensation in a double-layer graphene system very improbable.

The analysis of the problem presented in this paper is largely based on Ref. [28], in which a detailed theory of excitonic condensation in a single-layer graphene subject to the parallel magnetic field was developed. Although here we mainly concentrate on obtaining an analytical estimate for the transition temperature, many of the fine features of the excitonic state studied in Ref. [28] could be carried over to the double-layer graphene system.

2. Large- N approach to a double-layer graphene system

In this section, we will outline the main idea of the theoretical method, the large- N approximation, which will be used to obtain analytical estimates (2) and (4) for the transition temperature and the excitonic gap. For a double layer graphene system the large- N approximation appears to be particularly reliable and is expected to provide good quantitative predictions.

$$\begin{aligned}
& \text{~~~~~} = \\
& = \quad (1) \text{~~~~~} \sim r_s \quad + \quad (2) \text{~~~~~} \sim r_s^2 N \\
& \quad + \quad (3.1) \text{~~~~~} \sim r_s^3 N^2 \\
& + \quad (3.2) \text{~~~~~} \sim r_s^3 N \quad + \quad (3.3) \text{~~~~~} \sim r_s^3 N \\
& + \quad (4.1) \text{~~~~~} \sim r_s^4 N^3 \quad + \dots \\
& = \quad \text{~~~~~} + \text{~~~~~}
\end{aligned}$$

Figure 2. The idea of the large- N approximation. In each order in the bare Coulomb interaction (wavy lines), the leading in $N \gg 1$ diagrams for the effective interaction (“photon propagator”, double wavy line) are those that contain the maximum number of fermionic loops. So, in the third order [diagrams (3.1)-(3.3)], the diagrams (3.2) and (3.3) are smaller than (3.1) in $1/N \ll 1$ and can be neglected. Performing the same analysis for higher orders, one arrives at the series analogous to that of the RPA. The summation of this series can be reduced to solving an equation for the effective interaction (last line).

The bare strength $r_s = e^2/(\varepsilon v)$ (e is the electron charge, ε is the dielectric constant of the insulating medium surrounding graphene, $v \approx 10^8 \text{ cm/s}$ is the velocity of the Dirac spectrum, and we will use the units, in which the Planck’s constant $\hbar = 1$ throughout the paper) of the Coulomb interactions in graphene is not that small. For graphene in vacuum ($\varepsilon = 1$) $r_s \approx 2.16$ and for SiO_2 as an insulator typically $r_s \approx 1$ or somewhat smaller. These values of r_s are not exceptionally large, but cannot be considered as small either. Therefore, strictly speaking, the weak-coupling treatment of the Dirac fermions in graphene for the realistic values of r_s is not applicable. In the diagrammatic approach, for $r_s \gtrsim 1$ one would have to sum up all diagrams in each order in the bare interaction. Clearly, this task cannot be carried out analytically. If, however, the number N of independent fermionic species, or “flavors” is large, one has an additional expansion parameter, which can efficiently be exploited. The flavors can correspond to, e.g., different projections of the real spin S of particles, in which case N would be the total number of possible spin projections, $N = 2S + 1$, or to some other effective discrete

degrees of freedom, which stem from the properties of the particles spectrum.

So, if the number of flavors N is indeed large, one can notice (Fig. 2) that after summing the contributions of all flavors (“performing the trace over the flavor indices”) each closed fermionic loop consisting of the fermionic Green’s functions gives the factor N . Therefore, in a given order in the bare interaction, the leading in $N \gg 1$ contribution to the effective interaction (“photon propagator”) comes from the diagrams with the maximum numbers of electron loops. These are the diagrams that contain only the polarization bubbles consisting of two Green’s functions. The series of such diagrams can already be summed up as it is *formally* identical to the one of the well-known Random Phase Approximation (RPA).

Physically, the leading in N series describes the effect of linear screening of interactions by the carriers. Of course, screening is to some extent present in any system of free charged particles. However, in the limit of large N screening is particularly strong, since *all* N species participate in the screening of the interactions between fermions of *each* particular species. Screening makes the system effectively weakly interacting reducing the coupling constant from r_s to $1/N$: $r_s \rightarrow 1/N$. This allows one to study the system analytically, despite the fact that the bare Coulomb interactions may be not weak ($r_s \gtrsim 1$).

How large is the number of flavors N in a double-layer graphene system (Fig. 1)? In a single layer of graphene the number of species is equal to

$$N_1 = N_s N_v = 4$$

due to $N_s = 2$ possible projections of spin and $N_v = 2$ valleys. The large- N approach to a single-layer graphene was used in a number of works [28, 29, 30, 31, 32, 33, 34, 35, 36] before. For a double-layer system one has an additional “which-layer” degree of freedom, since each carrier can belong to either one of the layers. This twofold ($N_l = 2$) degeneracy appears formally in calculations when summing the polarization bubbles of both layers. Therefore, in a double-layer graphene system (Fig. 1) the total number of flavors is equal to

$$N = N_s N_v N_l = 2^3 = 8. \quad (5)$$

For this value it is quite reasonable to expect the large- N approximation to give good quantitative predictions. The accuracy of the obtained results will be estimated below in Sec. 4.

So, with $N = 8$ the large- N approximation seems to be particularly suitable for the double-layer graphene system. On the one hand, this is an attractive situation for theorists, since one is able to perform analytical calculations and make reliable quantitative predictions for a system of non-weakly interacting electrons. On the other hand, since the system is effectively in the weak coupling regime, one could expect the transition temperature to be quite small, which certainly is a pessimistic prospective for experimentalists trying to observe excitonic condensation in such a system.

Before we proceed with calculations, we would like to emphasize one important point. Although the diagrammatic series in RPA and large- N approximation are

formally identical, there is an important difference in the validity of the two approaches. The RPA works, when the characteristic energies ϵ and momenta q (set, e.g., by temperature) of the excitations contributing to the studied quantity are small compared to the Fermi scale: $\epsilon \ll \epsilon_F$ and $q \ll p_F$. The reason for that is the possibility to describe the low-energy excitations in terms of the charge and spin densities, quadratic in the fermionic operators. On the other hand, the large- N approximation is applicable as long as $N \gg 1$ and does not require the smallness of the relevant energy scales compared to the Fermi energy. It works even when the Fermi surface is absent in the problem, e.g., in the vicinity of the Dirac point in graphene[28, 29, 30, 31, 32, 33, 34, 35, 36]. Actually, as we will see in the next section, the excitonic gap and the transition temperature are determined by all transfer momenta q in the range $0 \leq q \leq 2p_F$, where p_F is the Fermi momentum. Therefore, strictly speaking, the RPA does not apply to the problem when the bare interactions are not weak. It does, however, apply to the case of weak bare interactions and we will come back to this point, when we discuss the transition temperature in more detail in Sec. 4.

3. Gap equation

In this section, we present the self-consistency equation for the excitonic gap, which will be used in the next two sections to obtain the mean-field temperature and the gap in the excitonic state.

To study the excitonic condensation in a double-layer graphene system (Fig. 1) we will use the following electron Hamiltonian,

$$\hat{H} = \sum_{i=e,h} \hat{H}_0^i + \sum_{i,j=e,h} \hat{H}_{\text{int}}^{ij}. \quad (6)$$

Here, the indices i and j numerate electron (e) and hole (h) layers. The terms

$$\hat{H}_0^i = \int d\mathbf{r} \hat{\phi}_i^\dagger(\mathbf{r})(v\boldsymbol{\tau}\mathbf{p} - \mu_i)\hat{\phi}_i(\mathbf{r}) \quad (7)$$

describe the free Dirac particles in graphene layers, where $\hat{\phi}_i(\mathbf{r})$ are the Dirac spinor field operators, \mathbf{r} is a two-dimensional radius vector in graphene layers, $\mathbf{p} = -i\nabla_{\mathbf{r}}$ is the momentum operator, and $\boldsymbol{\tau} = (\tau_x, \tau_y)$ is a vector consisting of the Pauli matrices τ_x and τ_y in the sublattice space of graphene honeycomb lattice. The chemical potentials $\mu_{e,h}$ of electrons and holes have opposite signs and will be assumed equal in absolute value,

$$\mu_e = -\mu_h = \epsilon_F.$$

This corresponds to the most favorable situation for the excitonic condensation, as any mismatch $\mu_e - |\mu_h|$ acts as an effective Zeeman field and tends to suppress the condensate. Further, the terms

$$\hat{H}_{\text{int}}^{ij} = \frac{1}{2} \int d\mathbf{r} d\mathbf{r}' \hat{\phi}_i^\dagger(\mathbf{r}) \hat{\phi}_j^\dagger(\mathbf{r}') V_{ij}(\mathbf{r} - \mathbf{r}') \hat{\phi}_j(\mathbf{r}') \hat{\phi}_i(\mathbf{r}) \quad (8)$$

in Eq. (6) describe the intralayer ($i = j$) and interlayer ($i \neq j$) Coulomb interactions between the Dirac particles with $V_0(\mathbf{r}) = V_{ee}(\mathbf{r}) = V_{hh}(\mathbf{r})$ and $V_1(\mathbf{r}) = V_{eh}(\mathbf{r}) = V_{he}(\mathbf{r})$ given by the Coulomb potential

$$V_0(\mathbf{r}) = \frac{e_*^2}{|\mathbf{r}|}, \quad V_1(\mathbf{r}) = \frac{e_*^2}{\sqrt{|\mathbf{r}|^2 + d^2}}, \quad (9)$$

In Eq. (9), e_* is an effective electron charge screened by the insulator embedding graphene sheets, $e_*^2 = e^2/\varepsilon$, and d is the distance between the layers.

The order parameter of the excitonic condensate is defined as

$$\hat{\Delta}(\mathbf{n}) = \int d\mathbf{r} e^{-ip_F \mathbf{n}(\mathbf{r}-\mathbf{r}')} V_1(\mathbf{r}-\mathbf{r}') \langle \hat{\phi}_e(\mathbf{r}) \hat{\phi}_h^\dagger(\mathbf{r}') \rangle. \quad (10)$$

Here, \mathbf{n} is the unit vector representing the direction of the electron momentum on the Fermi surface. In the sublattice space $\hat{\Delta}(\mathbf{n})$ has the following matrix structure,

$$\hat{\Delta}(\mathbf{n}) = \Delta \bar{\mathcal{P}}(\mathbf{n}) + \Delta' \bar{\mathcal{P}}(-\mathbf{n}), \quad (11)$$

where $\bar{\mathcal{P}}(\mathbf{n}) = (i\tau_z + \boldsymbol{\tau}\mathbf{t})/2$ and $\mathbf{t} = (-n_y, n_x)$ is the vector orthogonal to $\mathbf{n} = (n_x, n_y)$ in the xy plane. The constant Δ is the excitonic gap of the spectrum, $\epsilon_p = \sqrt{\Delta^2 + \xi^2}$, $\xi = v(p - p_F)$. The physical quantities of the condensate are determined by Δ , whereas the other constant in Eq. (11), Δ' , which is related to Δ , does not enter any of them. The properties of the excitonic gap Δ will be of our main interest from now on.

Within the large- N approach, the theory is analogous to the conventional weak-coupling Bardeen-Cooper-Schrieff (BCS) theory with the interaction given by the screened interlayer Coulomb potential. The equation for the excitonic gap Δ has the conventional BCS-like form [28]

$$\Delta = \lambda_\Delta T \sum_{n=-\infty}^{+\infty} \int_{-\epsilon_F}^{+\epsilon_F} d\xi \frac{\Delta}{\varepsilon_n^2 + \xi^2 + \Delta^2}. \quad (12)$$

In Eq. (12), T is the temperature, $\varepsilon_n = \pi T(2n + 1)$ are the fermionic Matsubara frequencies and the summation should be carried out over all integer n . The integration over ξ , which diverges logarithmically if the summation over n is performed first, should be cut by the Fermi energy $\pm\epsilon_F$. Further, the dimensionless coupling constant of the screened interlayer Coulomb interactions is given by the expression

$$\lambda_\Delta = \nu \int_0^{2\pi} \frac{d\theta}{2\pi} V_\Delta \left(2p_F \sin \frac{\theta}{2} \right) \frac{1 + \cos \theta}{2}, \quad (13)$$

where $\nu = \epsilon_F/(2\pi v^2)$ is the density of states in each graphene layer per one projection of spin and one valley. In Eq. (13), $V_\Delta(q)$ is the Fourier component of the static (at frequency $\omega = 0$) screened interlayer Coulomb interaction potential. The static limit for the coupling potential is valid with the logarithmic accuracy. The potential $V_\Delta(q)$ depends on the value of the gap Δ , since screening is affected by the presence of the excitonic gap. We will discuss the latter point in detail and present the explicit expression for $V_\Delta(q)$ in the excitonic phase in Sec. 5.

Two important points should be emphasized about Eqs. (12) and (13). First, as follows from Eq. (13), the coupling strength λ_Δ is determined by all transfer momenta

$q = 2p_F \sin(\theta/2)$ in the range $0 \leq q \leq 2p_F$, or equivalently, by all scattering angles in the range $0 \leq \theta \leq 2\pi$. This integration over the scattering angles is standard and it also appears in the conventional BCS theory. This fact is, however, crucial for obtaining the correct estimate for the gap Δ in the excitonic state. It will be key to disproving the statement made in Ref. [27] that, in terms of its effect on the magnitude of the gap, screening is suppressed in the excitonic state.

The second point is the presence of the factor $(1 + \cos \theta)/2$ in Eq. (13). It stems from the chiral nature of Dirac fermions in graphene and leads to the suppression of backscattering. This feature is specific to graphene and is absent in the system with conventional electronic spectrum. So, for any point-like interaction, $V_\Delta(q) = U_0 = \text{const}$, the coupling strength $\lambda_\Delta = \nu U_0/2$ is actually two times smaller than the conventionally defined dimensionless coupling constant νU_0 . As the transition temperature following from Eq. (12) depends on λ_Δ exponentially (see next section), this reduction by the factor 2 leads to an additional substantial suppression of the transition temperature compared to the double layer system with the conventional electronic spectrum.

Equations (12) and (13) supplemented by the proper form of the interlayer Coulomb potential $V_\Delta(q)$ allow one to obtain an analytical estimate for the transition temperature and the excitonic gap. In the next section we will calculate the mean field transition temperature. The results of the next section reproduce those of Ref. [26].

4. Mean-field transition temperature

In order to find the mean field transition temperature T_c , one needs to linearize the gap equation (12) in Δ and determine the temperature at which a nonzero solution to it appears. Calculating the integral over ξ and the sum over n in the linearized Eq. (12), one arrives at the BCS-like expression

$$T_c \approx \exp(-1/\lambda_{\Delta=0})\epsilon_F. \quad (14)$$

In Eq. (14), the screened Coulomb potential $V_{\Delta=0}(q)$ [see Eq. (13) for $\lambda_{\Delta=0}$] should be determined in the normal state, when $\Delta = 0$.

Calculating the potential $V_{\Delta=0}(q)$ in the large- N approximation is formally analogous to the RPA. One important difference, however, is that since the relevant transfer momenta $q = 2p_F \sin \theta/2$ belong to the range $0 \leq q \leq 2p_F$ [Eq. (13)], one has to use the exact expression for the polarization operator $\Pi_\Delta(\omega, q)$, and not its approximate form at $q \ll p_F$. However, the static polarization operator $\Pi_{\Delta=0}(q) = \Pi_{\Delta=0}(\omega = 0, q)$ in the normal state in graphene [34, 37] does not depend on momentum q at all in this range and equals

$$\Pi_{\Delta=0}(q) = N_s N_v \nu, \quad q \leq 2p_F. \quad (15)$$

The expressions for the bare intralayer and interlayer Coulomb interaction potentials [Eq.(9)] in the Fourier representation read

$$V_0(q) = \frac{2\pi e_*^2}{q}, \quad V_1(q) = \frac{2\pi e_*^2 \exp(-qd)}{q}, \quad (16)$$

respectively. Using Eqs. (15) and (16) and performing analogous to the RPA calculations one obtains for the screened interlayer Coulomb potential in the normal state

$$V_{\Delta=0}(q) = \frac{2\pi e_*^2 \exp(-qd)}{q + 2\kappa + \kappa^2[1 - \exp(-2qd)]/q}, \quad q \leq 2p_F. \quad (17)$$

In Eq. (17),

$$\kappa = 2\pi N_s N_v e_*^2 \nu \quad (18)$$

is the Debye screening wavevector (inverse screening length) in each layer.

Substituting Eq. (17) into Eq. (13), one obtains the mean field transition temperature T_c from Eq. (14). Let us estimate the highest possible value of T_c . According to Eq. (17) the potential $V_{\Delta=0}(q)$ is maximal, when the interlayer spacing d satisfies the condition

$$\kappa d \ll 1. \quad (19)$$

The other required condition, $p_F d \ll 1$, is automatically satisfied for $r_s \gtrsim 1$ in the limit (19), since $\kappa = r_s N_s N_v p_F = 4r_s p_F$. In reality, the limit (19) is hardly achievable. Indeed, on the one hand, one would like to have a large Fermi energy ϵ_F to have a higher cutoff energy in Eq. (14), but on the other hand, higher ϵ_F would require very smaller interlayer distance d . For $\epsilon_F = 0.3\text{eV}$ and $r_s = 1$, the condition (19) corresponds to $d \ll 0.5\text{ nm}$.

So, in the limit (19) of “zero” interlayer distance d , the interlayer potential (17) is maximal and equals

$$V_{\Delta=0}^{\max}(q) = \frac{2\pi e_*^2}{q + 2\kappa}. \quad (20)$$

Equation (20) has the same form as the screened Coulomb potential of a single layer. Note, however, the factor 2 in the term 2κ in Eq. (20). It originates from summing the polarization operators of both layers and reflects the above discussed “which-layer” degeneracy ($N_l = 2$), while the Debye wavevector κ [Eq. (18)] contains the spin ($N_s = 2$) and valley ($N_v = 2$) degeneracies of each layer. One may say that screening in a double-layer system is twice as efficient as in a single layer, since the carriers of both layers participate in it. The potential $V_{\Delta=0}^{\max}(q)$ is a decreasing function of q with the maximum at $q = 0$. Using Eq. (18) we obtain

$$\nu V_{\Delta=0}^{\max}(q = 0) = \frac{1}{N} = \frac{1}{8}. \quad (21)$$

We see that the maximum (21) of the dimensionless coupling constant is given by the inverse number of flavors and is, therefore, small for large N . Inserting Eq. (21) into Eq. (13), one obtains the maximum possible value of the coupling constant $\lambda_{\Delta=0}$ in the normal state:

$$\lambda_{\Delta=0}^{\max} = \frac{1}{2N} = \frac{1}{16}. \quad (22)$$

As discussed above, the coupling constant $\lambda_{\Delta=0}^{\max}$, which determines the transition temperature, is twice as small as the one given by Eq. (21) due to the suppression

of backscattering. Inserting Eq. (22) into Eq. (14), one obtains the maximum possible value of the mean-field transition temperature,

$$T_c^{\max} \approx \exp(-2N)\epsilon_F = \exp(-16)\epsilon_F \approx 10^{-7}\epsilon_F. \quad (23)$$

We see that, although the value $\lambda_{\Delta=0}^{\max}$ [Eq. (22)] is not particularly small, the mean-field temperature appears to be extremely small due to its exponential dependence on $\lambda_{\Delta=0}^{\max}$. With $\epsilon_F \sim 0.3\text{eV}$, Eq. (23) corresponds to $T_c^{\max} \sim 1\text{mK}$.

Let us here emphasize the difference between the large- N approximation and the RPA in connection to the considered problem. Basically, Eqs. (12) and (13) of the weak-coupling BCS-like theory are valid whenever the dimensionless coupling constant λ_{Δ} of the screened interlayer Coulomb interactions is small. In case of a sufficiently large number N of flavors the coupling constant $\lambda_{\Delta=0}^{\max}$ [Eq. (22)] is small in $1/N \ll 1$ and the applicability of the weak-coupling theory [Eqs. (12) and (13)] is justified for arbitrary strength of the bare interactions. However, if the number of flavors were not large (e.g., if $N_s = N_v = 1$), Eqs. (12) and (13) would still be valid in the weak coupling regime of the bare interlayer interaction $V_1(q)$, i.e., when $r_s \ll 1$ or $p_F d \ll 1$, see Eq. (16). Indeed, in the integral over $q = 2p_F \sin(\theta/2)$ in Eq. (13), $\nu V_1(q \sim p_F) \sim r_s \ll 1$ in the major range of integration $q \sim p_F$, and for these q the bare interaction potential is weak. Only for $q \ll p_F$ the bare coupling $\nu V_1(q \ll p_F) \gtrsim 1$ is not small. But for small $q \ll p_F$ the RPA is valid and the effective interaction is described by Eq. (17), in which the number of flavors N does not need to be large. Actually, the gap equations (12), (13), and (17) were obtained in Refs. [20, 21] in limit of weak interlayer interactions ($r_s \ll 1$ or $p_F d \ll 1$) within the RPA approximation before Eq. (14) for the mean-field temperature was derived in Ref. [26] using the large- N approximation. An important conclusion of Ref. [26] is that due to the reasonably large numerical value $N = 8$, these equations are valid and provide reliable quantitative prediction for T_c not only for weak interlayer interactions, but also in the realistic case of moderate to strong interactions, when $r_s \gtrsim 1$.

Let us estimate the accuracy of the result (23). This equation is obtained by taking into account the leading in N diagrams (Fig. 2) for the effective interlayer interaction. The diagrams that are neglected [such as diagrams (3.2) and (3.3) compared to (3.1)] are smaller in $1/N$ than the leading contribution. Therefore, one could represent the exact coupling constant $\lambda_{\Delta=0}^{\max}$ in the form of an asymptotic series in N with Eq. (22) giving the leading term of the series. This way, one can write down the inverse coupling constant as

$$1/\lambda_{\Delta=0}^{\max} = 2N - \mathcal{O}(1), \quad (24)$$

where $\mathcal{O}(1) > 0$ represents all subleading in $1/N$ terms and is of order unity, $\mathcal{O}(1) \sim 1$.

Inserting Eq. (24) into the exponential function in Eq. (14) one can conclude that in the best case scenario the transition temperature T_c^{\max} could be about one order ($e^{\mathcal{O}(1)}$) greater than the one given by Eq. (23). With the proper (yet unknown within the logarithmic accuracy) numerical prefactor in Eq. (23) one could optimistically hope that T_c^{\max} could reach 100mK for $\epsilon_F \sim 0.3\text{eV}$. Unfortunately, what concerns the possibility to

observe the effect experimentally, this would not radically change the situation. First, as it was mentioned, the maximum (22) of the interaction strength is virtually unachievable in the experiment, since this requires the condition (19) to be satisfied. Second, as it will be discussed in Sec. 6, inevitable boundary scattering at the edges of graphene sheets will destroy any condensate with $T_c \lesssim 1\text{K}$ even in a system free of any bulk disorder.

5. Excitonic gap and screening in the excitonic state

In addition to the mean field temperature T_c obtained in the previous section, one can estimate the Berezinski-Kosterlitz-Thouless (BKT) transition temperature. The BKT transition [24, 25] occurs in two-dimensional superfluid systems, in which thermal fluctuations destroy the long-range order of the order parameter. The BKT temperature is defined as the temperature at which creation of topological defects (most commonly, vortices) in the order parameter becomes thermodynamically favorable. Mathematically, this condition can be expressed as:

$$\frac{\pi}{2}\rho(T_{KT}) = N_{KT}T_{KT}, \quad (25)$$

where $\rho(T)$ is the so-called stiffness of the order parameter, which determines the energy of the topological defect. The factor $N_{KT} = 1$ for vortices. As shown in Ref. [28], however, in graphene creation of halfvortices can be more favorable, in which case $N_{KT} = 4$ and T_{KT} would be somewhat lower than for $N_{KT} = 1$. Within the mean-field theory, the stiffness has the form [28]

$$\rho(T) = \frac{\epsilon_F}{4}T \sum_{n=-\infty}^{+\infty} \frac{\Delta^2(T)}{[\epsilon_n^2 + \Delta^2(T)]^{3/2}}, \quad (26)$$

where $\Delta(T)$ is the excitonic gap, which should be obtained by solving the gap equation (12). The stiffness (26) takes a universal value $\rho(T=0) = \epsilon_F/(4\pi)$ at low temperatures, when $T \ll \Delta(T)$, decreases with increasing temperature, and vanishes when T approaches the mean-field temperature (14), $T \rightarrow T_c$, where the gap turns to zero, $\Delta(T_c) = 0$. Therefore, the BKT temperature T_{KT} , which is a solution of Eq. (25), cannot exceed the mean-field temperature T_c ,

$$T_{KT} < T_c. \quad (27)$$

This is illustrated graphically in Fig. 3. The result (27) is also intuitively clear, since one would naturally expect thermal fluctuations of the order parameter to suppress, rather than enhance, the superfluidity of the system.

One can conclude from Eq. (27) that the estimate (2), obtained within the mean-field approach, sets the upper bound for the temperature of any realistic [28] phase transition into the excitonic state in a double-layer graphene system. Nevertheless, as mentioned in the introduction, the authors of Ref. [27] came to quite a different conclusion. On the one hand, they agreed \ddagger that the mean-field temperature T_c indeed

\ddagger The authors of Ref. [27] actually provided an estimate $T_c \sim 6 \cdot 10^{-5} \epsilon_F$ for the mean-field temperature, which is more than two orders greater the result (2) for the highest possible value of T_c . It is hard to

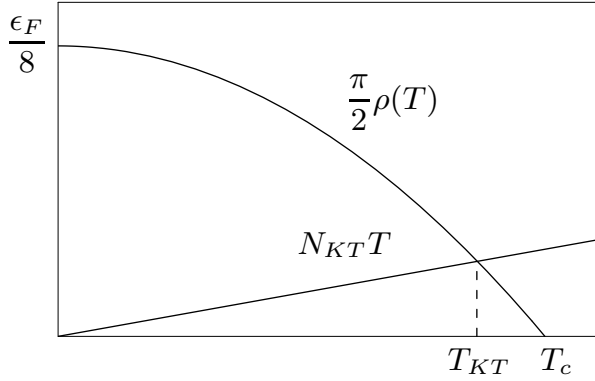


Figure 3. Graphical solution of Eq. (25) for the BKT transition temperature T_{KT} . The stiffness $\rho(T)$ [Eq. (26)] of the order parameter takes a universal value $\rho(T=0) = \epsilon_F/(4\pi)$ at low temperatures (when $T \ll \Delta(T)$) decreases with increasing temperature T , and vanishes at the mean-field transition temperature $T = T_c$, where the excitonic gap $\Delta(T = T_c) = 0$ turns to zero. Therefore, the BKT temperature T_{KT} cannot exceed the mean-field temperature T_c , Eq. (27).

appears to be significantly smaller than their initial estimate T_{KT}^* [Eq. (1)] for the BKT temperature, provided screening is taken into account. On the other hand, they argued that in the excitonic phase the gap in the excitation spectrum suppresses screening, which would mean that the gap $\Delta^*(T)$ itself should be of the same order as the estimate (1) obtained neglecting screening, see Eq. (3). Such a strong discrepancy between T_c [Eq. (2)] and $\Delta^*(T=0)$ [Eq. (3)] indicates, according to Ref. [27], that the system should undergo a first-order transition into the excitonic state at temperature $T \sim \Delta^*(T=0)$, which would again correspond to high temperatures.

We will now show that, in fact, the other, less exciting, scenario is realized. We will demonstrate that the suppression of screening by the gap in the excitonic state, although it does take place, has a negligible effect on the value of the gap, when the latter is determined self-consistently from the gap equations (12) and (13). As a result, the system is in the weak-coupling regime of the screened interactions, described by the large- N approximation, at all temperatures below T_c and the value of the gap $\Delta(T) \lesssim 10^{-7}\epsilon_F$ in the excitonic state appears to be in full agreement with the value (2) of the mean-field temperature.

To prove this point, one needs the expression for the screened interlayer Coulomb potential $V_\Delta(q)$ in the excitonic phase, where $\Delta \neq 0$. Performing the calculations analogous to those of RPA, in the large- N approximation one obtains

$$V_\Delta(q) = \frac{V_+(q)}{1 + 2\Pi_\Delta^+(q)V_+(q)} - \frac{V_-(q)}{1 + 2\Pi_\Delta^-(q)V_-(q)}. \quad (28)$$

Here

$$V_\pm(q) = \frac{1}{2}[1 \pm \exp(-qd)] \frac{2\pi e_*^2}{q} \quad (29)$$

comment on the possible origin of this discrepancy, since no analytical formula for T_c was presented in Ref. [27].

are the half-sum and half-difference of the intralayer $V_0(q)$ and interlayer $V_1(q)$ bare Coulomb potentials [Eq. (16)]. The polarization operators

$$\Pi_{\Delta}^{\pm}(q) = \Pi_{\Delta}^0(q) \pm \Pi_{\Delta}^1(q) \quad (30)$$

in Eq. (28) are the sum and difference of the intralayer $\Pi_{\Delta}^0(q)$ and interlayer $\Pi_{\Delta}^1(q)$ polarization operators. The operators $\Pi_{\Delta}^0(q)$ and $\Pi_{\Delta}^1(q)$ describe the density response in one layer to the density perturbation in the same and other layer, respectively, and can be written down in the Matsubara representation [38] as

$$\Pi_{\Delta}^{0,1}(q) = \int_0^{1/T} d\tau \int d\mathbf{r} e^{-i\mathbf{q}\mathbf{r}} \langle \hat{\rho}_i(\tau, \mathbf{r}) \hat{\rho}_j(0, 0) \rangle \quad (31)$$

with the same layer indices ($i = j$) for $\Pi_{\Delta}^0(q)$ and different ones ($i \neq j$) for $\Pi_{\Delta}^1(q)$. In Eq. (31), $\hat{\rho}_i(\mathbf{r}) = \hat{\phi}_i^{\dagger}(\mathbf{r})\hat{\phi}_i(\mathbf{r})$ are the density operators and τ is the Matsubara time.

The polarization operators (31) can be calculated using the Green's functions for the excitonic state. Doing so, one obtains that in the excitonic state $\Pi_{\Delta}^{-}(q)$ does not depend on the gap at all and is equal to its normal state value

$$\Pi_{\Delta}^{-}(q) = N_s N_v \nu. \quad (32)$$

On the hand, the operator $\Pi_{\Delta}^{+}(q)$ is affected by the gap and the expression for it reads

$$\Pi_{\Delta}^{+}(q) = N_s N_v \nu \left\{ 1 - \pi T \sum_{n=-\infty}^{+\infty} \int_0^{2\pi} \frac{d\theta}{2\pi} \frac{\Delta^2}{[(\varepsilon_n^2 + \Delta^2) + (vq \cos \theta)^2/4] \sqrt{\varepsilon^2 + \Delta^2}} \right\} \quad (33)$$

Here, as in Eq. (12), $\varepsilon_n = \pi T(2n + 1)$ are the fermionic Matsubara frequencies and the summation is done over all integer n .

Aiming to find the highest possible value of the gap, let us again consider the limit (19) of “zero” interlayer distance, when the potential $V_{\Delta}(q)$ [Eq. (28)] is maximal. In this limit the second term in Eq. (28) can be neglected, $V_+(q) = V_0(q)$ [Eqs. (16) and (29)], and the interlayer interaction potential takes the form

$$V_{\Delta}^{\max}(q) = \frac{V_0(q)}{1 + 2\Pi_{\Delta}^{+}(q)V_0(q)}. \quad (34)$$

Again, as in Eq. (20), the factor 2 in the denominator in Eq. (34) originates from summing the polarization operators of both layers.

Let us discuss the properties of the polarization operator (33) and the corresponding properties of the potential (34). In the normal state ($\Delta = 0$), the second term in Eq. (33) is zero, $\Pi_{\Delta=0}^{+}(q)$ is given by Eq. (15) and one recovers the expression (20) for $V_{\Delta=0}^{\max}(q)$ from Eq. (34). The second term in Eq. (33) exists in the excitonic phase only, when $\Delta \neq 0$. It is a decreasing function of q and approaches zero for $q \gg \Delta/v$ exceeding the condensate momentum Δ/v . So, for momenta $q \gg \Delta/v$ the polarization operator

$$\Pi_{\Delta}^{+}(q \gg \Delta/v) \approx N_s N_v \nu \quad (35)$$

is given by its normal state value (15) at any temperature, including $T = 0$, and the interlayer interaction potential is completely screened,

$$\nu V_{\Delta}^{\max}(q \gg \Delta/v) \approx \frac{1}{N}. \quad (36)$$

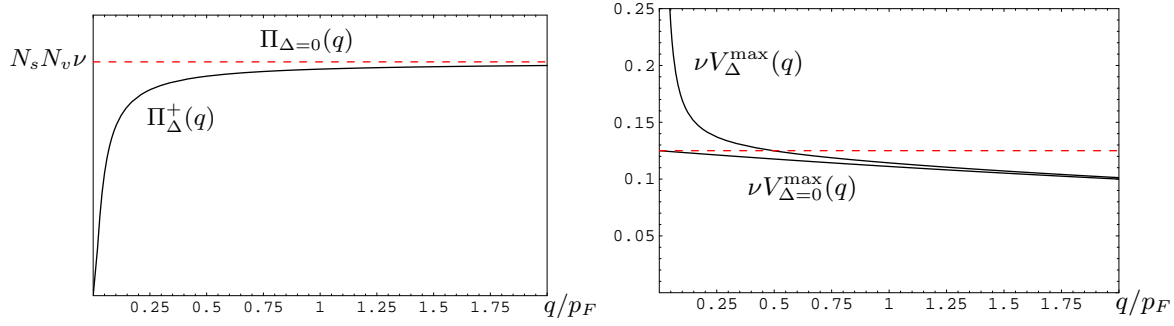


Figure 4. Dependence of the polarization operator $\Pi_{\Delta}^{+}(q)$ [Eq. (33), left graph] and the maximum of the screened interlayer potential $V_{\Delta}^{\max}(q)$ [Eq. (34), right graph] on momentum q in the excitonic state. The case of $\Delta/\epsilon_F = 10^{-2}$, $r_s = 1$, and zero temperature is shown. The operator $\Pi_{\Delta}^{+}(q)$ is suppressed for $q \lesssim \Delta/v$ below the condensate momentum Δ/v , whereas for greater $q \gg \Delta/v$ it approaches the normal-state value $\Pi_{\Delta=0}(q) = \nu N_s N_v$ [Eq. (15), dashed line]. Consequently, the potential $\nu V_{\Delta}^{\max}(q)$ is unscreened and exceeds its small normal-state value $\nu V_{\Delta=0}^{\max}(q) \leq 1/8$ [Eqs. (20) and (21)] only for $q \lesssim \Delta/v$. As the excitonic gap Δ is determined by all momenta in the range $0 \leq q \leq 2p_F$, see Eqs. (12) and (13), the suppression of screening at $q \lesssim \Delta/v$ gives only a minor correction to the coupling strength λ_{Δ} , which is small in the ratio Δ/ϵ_F [Eq. (39)].

Therefore, an important conclusion that can be drawn from Eqs. (35) and (36) is that for momenta q exceeding the condensate momentum Δ/v screening is just as strong in the excitonic state as it is in the normal state.

At the same time, the situation is different for small momenta. The polarization operator $\Pi_{\Delta}^{+}(q)$ is indeed suppressed at $q \lesssim \Delta/v$, when the second term in Eq. (33) contributes considerably. The smaller q and T are, the stronger the suppression of $\Pi_{\Delta}^{+}(q)$ is. In fact, at zero temperature $T = 0$ and zero momentum $q = 0$ the second term in Eq. (33) cancels the first term exactly and one gets

$$\Pi_{\Delta}^{+}(q = 0)|_{T/\Delta=0} = 0. \quad (37)$$

This means that at small momenta and low temperature screening is indeed suppressed and the interlayer Coulomb potential is unscreened,

$$V_{\Delta}^{\max}(q \lesssim \Delta/v)|_{T \ll \Delta} \approx \frac{2\pi e^2}{q}. \quad (38)$$

Equation (37) has a simple physical interpretation: at zero momentum and temperature all electrons and holes are paired into dipoles and there are no free carriers (excitations) that could screen the interaction.

The dependence of the polarization operator $\Pi_{\Delta}^{+}(q)$ [Eq. (33)] and of the interaction potential $V_{\Delta}^{\max}(q)$ [Eq. (34)] on q , illustrating the above properties, is plotted in Fig. 4.

It is essentially the property (37) of the polarization operator (33) that the authors of Ref. [22] used in Ref. [27] to argue that, in terms of its effect on the value of the gap Δ , screening should be suppressed. The expression (33) at $q = 0$ can be rewritten in the form of Eq. (4) of Ref. [27] using the conventional method [38] of replacing

the sum over the Matsubara frequencies ε_n by the integral over a continuous energy variable. According to Ref. [27], the property (37) justifies the neglect of screening, when determining the value of the gap in the condensed phase.

It is easy to understand now from Eqs. (12), (13), (33) and (34), and the discussed properties of the polarization operator (33) that the suppression of screening at small momenta $q \lesssim \Delta/v$ has a very little, in fact, negligible effect on the value of the gap. Indeed, as follows from Eq. (13) and was pointed out earlier in Sec. 3, the coupling strength λ_Δ and, consequently, the gap Δ [Eq. (12)], is determined by all scattering momenta $q = 2p_F \sin \theta/2$ in the range $0 \leq q \leq 2p_F$. As we have just discussed, screening is suppressed by the gap in the range $0 \leq q \lesssim \Delta/v$ only [Eqs. (37) and (38)], whereas in the range $\Delta/v \lesssim q \leq 2p_F$ screening is just as strong as in the normal state [Eqs. (35) and (36), Fig. 4]. Therefore, the difference

$$\delta\lambda_\Delta = \lambda_\Delta - \lambda_{\Delta=0}$$

between the pairing constant λ_Δ [Eq. (13)] in the condensed phase and its value $\lambda_{\Delta=0}$ in the normal state comes from the range of momenta $0 \leq q \lesssim \Delta/v$ only and is small in the ratio of the gap Δ to the Fermi energy $\epsilon_F = vp_F$,

$$\delta\lambda_\Delta/\lambda_{\Delta=0} \sim \Delta/\epsilon_F. \quad (39)$$

Equation (39) shows unambiguously that the presence of the excitonic gap does not influence the value of the coupling constant as long as $\Delta \ll \epsilon_F$. In other words, the statements of Ref. [27] cannot be correct unless the excitonic gap becomes of the order of the Fermi energy.

Let us now find the maximum value Δ_0^{\max} [in the limit (19) of “zero” interlayer distance] of the gap $\Delta_0 = \Delta(T = 0)$ at zero temperature, when the suppression of screening by the gap is greatest. From Eq. (12), one obtains that Δ_0 satisfies the equation

$$\Delta_0 \approx \exp(-1/\lambda_{\Delta_0}) \epsilon_F. \quad (40)$$

Unlike Eq. (14), which provides the explicit expression for the mean field transition temperature, one has to solve Eq. (40) to obtain Δ_0 , since λ_{Δ_0} depends on Δ_0 . However, considering the extremely small numerical value of T_c^{\max}/ϵ_F [Eq. (23)] we conclude immediately that

$$\Delta_0^{\max} \approx \exp(-1/\lambda_{\Delta=0}^{\max}) \epsilon_F = \exp(-16) \epsilon_F \approx 10^{-7} \epsilon_F, \quad (41)$$

for which the suppression of screening by the gap is neglected completely, is the solution of Eq. (40). Indeed, inserting the value (41) into Eq. (13) and calculating the integrals numerically, we obtain that $\delta\lambda_{\Delta_0}^{\max}/\lambda_{\Delta=0} \sim 10^{-6}$ [Eq. (39)], and therefore Δ_0^{\max} is determined by Eq. (41) with the relative precision $\sim 2N\delta\lambda_{\Delta_0}^{\max}/\lambda_{\Delta=0} \sim 10^{-4}$.

Besides Eq. (41), there are no other solutions to Eq. (40) in the range $\Delta_0 \lesssim \epsilon_F$, which can be checked numerically. One could use the highest hypothetical value (3) of the gap as the zeroth approximation, insert it into the right-hand side of Eq. (40), and obtain that already on the second iteration the solution collapses to the value (41) with high precision.

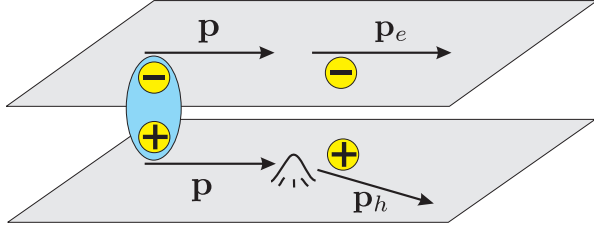


Figure 5. Sensitivity of the excitonic condensate to the impurity scattering. Impurities with the size of potential smaller than the interlayer distance scatter electrons and holes not identically, thereby breaking electron-hole pairs and suppressing the condensate.

We conclude that, contrary of the arguments of Ref. [27], in terms of its effect on the excitonic pairing, screening is as strong in the excitonic state as it is in the normal one. Partial suppression of screening at small momenta $q \lesssim \Delta/v$ has a negligible effect on the value of the gap when the latter is determined self-consistently from the gap equation. This clearly follows from the fact that all the scattering momenta q in the range $q \leq 2p_F$ contribute to the value of the gap, and not only small ones. Therefore, the normal-state expression (17) for the screened intralayer Coulomb potential can be used with great precision to study the excitonic phase at any temperature $T \leq T_c$ below the mean-transition temperature T_c (2). As a result, the maximum possible value of the zero-temperature gap (41) appears to be in full agreement with the result (2) for the mean field transition temperature. The fact that $\exp(-16)\epsilon_F \sim 10^{-7}\epsilon_F$ is the only energy scale of the excitonic pairing in the double-layer graphene system proves that Eq. (2) really sets the upper bound for the transition temperature and invalidates the conjecture of Ref. [27] about the high-temperature first order transition.

We would like to stress that all the above discussion about how screening is affected by the gap in the excitonic state was not actually in any way specific to graphene. The very same analysis could have been carried out for conventional systems [1, 2] with quadratic electron spectrum. What concerns graphene, the point that screening is only negligibly affected by the gap has been made earlier in Ref. [28], where the dependence of the polarization operator on Δ in the excitonic state (its suppression in the minor range of momenta $q \lesssim \Delta/v$) was neglected in the calculations for the reasons discussed above.

6. Influence of disorder

Although the estimate (2) predicts a really small value of the transition temperature, one could still hope to observe excitonic effects in a 1mK range. Unfortunately, in a realistic system even at these low temperatures the excitonic pairing could hardly be realized. The reason for this is that these estimates were made for a system that is free of any kind of disorder, while the excitonic condensate in double-layer systems is sensitive to the impurity scattering [39, 2]. Indeed, since the bound electron and hole carry the

same momentum \mathbf{p} , any scattering process that changes the momentum of electron and hole not identically, i.e., $\mathbf{p} \rightarrow \mathbf{p}_e$ for electron and $\mathbf{p} \rightarrow \mathbf{p}_h$ for hole, so that $\mathbf{p}_e \neq \mathbf{p}_h$, breaks the electron-hole pair (see Fig. 5). This is the case for impurities with the range of the scattering potential less than the interlayer distance d , since the potential of such impurities differs in the two layers. Therefore, any sufficiently strong-range impurities destroy the excitonic condensate.

Originally, the effect of the impurity scattering on the excitonic condensate was studied analytically for conventional systems in Refs. [39, 2]. The theory is formally analogous to the Abrikosov-Gorkov's theory [40] for magnetic impurities in superconductors. For a double layer graphene system, analogous calculations were performed in Ref. [41]. The main result is that sufficiently short-range impurities with the scattering time τ destroy the excitonic condensate completely as soon as

$$\tau T_c \lesssim 1, \quad (42)$$

where T_c is the transition temperature of the ideally clean system. Equivalently, for the condensate to exist, electron momentum has to be conserved at the scale of the correlation length v/T_c . How weak impurity scattering in a realistic system can be? Even if the system is free of bulk disorder, the mean free path is limited by the sample size due to the boundary scattering at the sample edges. With the typical size of graphene devices $\sim 1\mu\text{m}$ this corresponds to the scattering rate $1/\tau \sim 1\text{K}$. Therefore, we can conclude that any condensate with T_c in a clean system below 1K would be completely destroyed in a realistic system.

7. Comparison with conventional double-layer systems

In terms of engineering properties, the double-layer graphene system could seem as an exceptional candidate for the realization of the excitonic condensation. However, as we have seen in the previous sections, the peculiar properties of graphene spectrum (additional valley degrees of freedom and chirality) appear to play a negative role for this effect. To illustrate this point, let us estimate for comparison the highest possible value of the transition temperature in a double-layer system with the conventional quadratic electron spectrum, such as a semiconductor double quantum well, using the large- N approximation.

How should the equations of Sec. 3 be modified in this case? First, since the valley degeneracy $N_v = 2$ is absent, the total number of flavors is $N = N_s N_l = 4$ due to the two ($N_s = 2$) projections of spin and two layers ($N_l = 2$). Therefore, the maximum of the dimensionless coupling constant equals

$$\nu V_{\Delta=0}^{\max}(q=0) = \frac{1}{N} = \frac{1}{4} \quad (43)$$

Second, the factor $(1 + \cos \theta)/2$, which stems from the chiral nature of Dirac quasiparticles and results in the suppression of backscattering, is absent in Eq. (13).

Therefore, the maximum coupling strength $\lambda_{\Delta=0}^{\max}$ that determines the gap according to Eq. (12) is just equal to Eq. (43),

$$\lambda_{\Delta=0}^{\max} = \frac{1}{N} = \frac{1}{4}. \quad (44)$$

As we see, the pairing strength $\lambda_{\Delta=0}^{\max}$ in a double-layer with conventional spectrum is four times greater than the one in graphene-based system [Eq. (22)]. According to Eq. (14), for the maximum of the transition temperature one obtains

$$T_c^{\max} \approx \exp(-N)\epsilon_F = \exp(-4)\epsilon_F \approx 10^{-2}\epsilon_F. \quad (45)$$

This value is five orders higher than that for the graphene double-layer [Eq. (2)] and by no means does it lead to similar pessimistic conclusions about the feasibility of the effect. Of course, in this case the estimate (45) may already be quite crude because $\lambda_{\Delta=0}^{\max} = 1/4$ is not that small. However, this only indicates and the system could be on the verge of applicability of the weak-coupling limit and the actual T_c could be even higher than predicted by Eq. (45).

8. Excitonic condensation in a single-layer graphene

Besides a double-layer graphene system (Fig. 1), there were a couple of theoretical proposals how excitonic pairing could be realized in a single layer of graphene. We briefly discuss them in this section.

One possibility [28] would be to apply a strong in-plane magnetic field to a single layer of graphene. Such a field acts on the spins of the carriers only, and the Zeeman splitting creates electrons with one spin polarization and holes with the opposite polarization in an initially neutral sample. As electrons and holes in such a system have well-defined Fermi surfaces, the transition temperature can be estimated within the large- N approximation using Eqs. (12) and (13) of the BCS-like theory. The number of species in a single-layer graphene is $N_1 = N_s N_v = 4$ and the maximum of the coupling constant (13) equals to

$$\lambda_{\Delta=0}^{\max} = \frac{1}{2 N_s N_v} = \frac{1}{8} \quad (46)$$

The Zeeman splitting energy ϵ_Z plays the role of the Fermi energy in such a setup. Therefore, for the maximum of the transition temperature one obtains

$$T_c^{\max} \approx \exp(-\lambda_{\Delta=0}^{\max}) \epsilon_Z = \exp(-8) \epsilon_Z \approx 3 \cdot 10^{-4} \epsilon_Z \quad (47)$$

The exponential factor $\exp(-8)$ is not as small as $\exp(-16)$ in the double-layer system. However, the Zeeman splitting energy cannot be extremely high even for experimentally very high magnetic fields B . For $B \approx 40$ T one can estimate from Eq. (47) $T_c^{\max} \sim 20$ mK. Alternatively, instead of applying external magnetic field, one could bring the graphene sheet in contact with the ferromagnet, in which case the Zeeman splitting would be caused by the ferromagnet exchange field [28].

In the electrically biased double-layer graphene and a single-layer graphene in the parallel magnetic field electrons and holes have a finite density of states at the

mutual Fermi level. This way the excitonic pairing is realized through the Cooper instability mechanism, and a finite transition temperature formally exists for arbitrary small strength of the bare Coulomb interactions r_s (although, as it was demonstrated here, even for moderate to strong interactions the transition temperature appears to be numerically extremely small). It was conjectured in a number of works [33, 34, 35, 36] that the requirement of the finite DoS is actually not necessary and that excitonic pairing could be possible in an undoped graphene layer, with the chemical potential at the Dirac point. The analysis of Refs. [33, 34, 35, 36] predicts that opening of the excitonic gap at the Dirac point may occur, provided the Coulomb coupling strength $r_s = e^2/(\epsilon v)$ exceeds certain threshold value r_s^* . This value depends on the number of flavors and for $N = N_1 = 4$ equals $r_s^* = 2.33$, which is quite close to $r_s \approx 2.16$ in vacuum ($\epsilon = 1$).

9. Conclusion

We theoretically studied the possibility of excitonic condensation in a recently proposed double-layer graphene system. On the one hand, this system possesses several obvious engineering advantages compared to semiconductor double quantum wells, used so far experimentally. On the other hand, the properties of the graphene spectrum appear to be very unfavorable for realization of excitonic condensation in such a system. Additional valley degrees of freedom and suppression of backscattering in graphene lead to a much smaller value of the screened Coulomb interaction strength than in a system with conventional electron spectrum. It is shown the effect of screening on the excitonic pairing is just as strong in the excitonic state as it is in the normal state. For this reason, the value of the excitonic gap is found to fully agree with the previously obtained [26] estimate for the mean-field transition temperature, the maximum possible value $\sim 10^{-7}\epsilon_F$ of both being in the 1mK range for a perfectly clean system. These findings disprove the predictions [22, 23, 27] of the excitonic condensation at room temperatures and, unfortunately, render experimental observation of this undoubtedly interesting effect in a double-layer graphene system unlikely.

Acknowledgements

Insightful discussions with Igor Aleiner are greatly appreciated.

References

- [1] L. V. Keldysh and Yu. V. Kopayev, Sov. Phys. Solid State **6**, 2219 (1965).
- [2] Yu. E. Lozovik and V. I. Yudson, JETP Lett. **22**, 274 (1975); Sov. Phys. JETP **44**, 389 (1975); Solid State Commun. **19**, 391 (1976); Solid State Commun. **21**, 211 (1977).
- [3] U. Sivan, P. M. Solomon, and H. Shtrikman, Phys. Rev. Lett. **68**, 1196 (1992).
- [4] A. F. Croxall, K. Das Gupta, C. A. Nicoll, M. Thangaraj, H. E. Beere, I. Farrer, D. A. Ritchie, and M. Pepper Phys. Rev. Lett. **101**, 246801 (2008).
- [5] J. A. Seamons, C. P. Morath, J. L. Reno, and M. P. Lilly, Phys. Rev. Lett. **102**, 026804 (2009).

- [6] L. V. Butov, A. Zrenner, G. Abstreiter, G. Böhm, and G. Weimann, Phys. Rev. Lett. **73**, 304 (1994).
- [7] M. Bayer, V. B. Timofeev, F. Faller, T. Gutbrod, and A. Forchel, Phys. Rev. B **54**, 8799 (1996).
- [8] A. A. Dremin, V. B. Timofeev, A. V. Larionov, J. Hvam, and K. Soerensen, JETP Lett. **76**, 450 (2002).
- [9] L. V. Butov, C. W. Lai, A. L. Ivanov, A. C. Gossard, and D. S. Chemla, Nature **417**, 47 (2002).
- [10] L. V. Butov, A. C. Gossard, and D. S. Chemla, Nature **418**, 751 (2002).
- [11] I. B. Spielman, J. P. Eisenstein, L. N. Pfeiffer, and K. W. West, Phys. Rev. Lett. **84**, 5808 (2000); Phys. Rev. Lett. **87**, 036803 (2001);
- [12] J. P. Eisenstein and A. H. MacDonald, Nature **432**, 691 (2004).
- [13] K. S. Novoselov, A. K. Geim, S. V. Morozov, D. Jiang, Y. Zhang, S. V. Dubonos, I. V. Grigorieva, and A. A. Firsov, Science **306**, 666 (2004).
- [14] K.S. Novoselov, A.K. Geim, S.V. Morozov, D. Jiang, M.I. Katsnelson, I.V. Grigorieva, S.V. Dubonos, and A.A. Firsov, Nature **438**, 197 (2005).
- [15] Y. Zhang, J. P. Small, M. E. S. Amori, and P. Kim, Phys. Rev. Lett. **94**, 176803 (2005).
- [16] Y. Zhang, Y.-W. Tan, H. Stormer, and P. Kim, Nature **438**, 201 (2005).
- [17] C. Berger, Z. Song, T. Li, X. Li, A. Y. Ogbazghi, R. Feng, Z. Dai, A. N. Marchenkov, E. H. Conrad, P. N. First, and W. A. de Heer, J. Phys. Chem. B **108**, 19912 (2004).
- [18] C Berger, Z. Song, X. Li, X. Wu, N. Brown, C. Naud, D. Mayou, T. Li, J. Hass, A. N. Marchenkov, E. H. Conrad, P. N. First, and W. A. de Heer Science **312**, 1191 (2006).
- [19] A. K. Geim and K. S. Novoselov, Nat. Mater. **6**, 183 (2007).
- [20] Yu.E. Lozovik and A.A. Sokolik, JETP Lett. **87**, 55 (2008).
- [21] Yu. E. Lozovik, S. P. Merkulova, and A. A. Sokolik, Usp. Fiz. Nauk **178**, 757 (2008), in Russian.
- [22] H. Min, R. Bistritzer, J.-J. Su, and A.H. MacDonald, Phys. Rev. B **78**, 121401(R) (2008).
- [23] C.-H. Zhang and Y. N. Joglekar, Phys. Rev. B **77**, 233405 (2008).
- [24] V. L. Berezinskii, Sov. Phys. JETP **32**, 493 (1971).
- [25] J. M. Kosterlitz and D. J. Thouless, J. Phys. C **5**, L124 (1972).
- [26] M. Yu. Kharitonov and K. B. Efetov, Phys. Rev. B **78**, 241401 (2008).
- [27] R. Bistritzer, H. Min, J. J. Su, and A.H. MacDonald, arXiv:0810.0331, unpublished.
- [28] I. L. Aleiner, D. E. Kharzeev, and A. M. Tsvelik, Phys. Rev. B **76**, 195415 (2007).
- [29] J. Ye and S. Sachdev, Phys. Rev. Lett. **80**, 5409 (1998).
- [30] D. T. Son, Phys. Rev. B **75**, 235423 (2007).
- [31] M. S. Foster and I. L. Aleiner, Phys. Rev. B **77**, 195413 (2008).
- [32] M. Mueller, L. Fritz, and S. Sachdev, Phys. Rev. B **78**, 115406 (2008).
- [33] D. V. Khveshchenko, Phys. Rev. Lett. **87**, 206401 (2001); *ibid* **87**, 246802 (2001).
- [34] E. V. Gorbar, V. P. Gusynin, V. A. Miransky, and I. A. Shovkovy, Phys. Rev. B **66**, 045108 (2002); Phys. Lett. A **313**, 472 (2003).
- [35] D. V. Khveshchenko and H. Leal, Nucl. Phys. B **687**, 323 (2004); D. V. Khveshchenko and W. F. Shively, Phys. Rev. B **73**, 115104 (2006).
- [36] D. V. Khveshchenko, J. Phys.: Condens. Matter **21**, 075303 (2009).
- [37] B. Wunsch, T. Stauber, F. Sols, and F. Guinea, New J. Phys. **8**, 318 (2006).
- [38] A. A. Abrikosov, L. P. Gor'kov, and I. E. Dzyaloshinski, *Methods of Quantum Field Theory in Statistical Physics*, Prentice-Hall (1963).
- [39] J. Zittartz, Phys. Rev. **164**, 575 (1967).
- [40] A. A. Abrikosov and L. P. Gor'kov, Sov. Phys. JETP **12**, 1243 (1961).
- [41] R. Bistritzer and A.H. MacDonald, Phys. Rev. Lett. **101**, 256406 (2008).